Article

Ligand Binding in a Docking Site of Cytochrome *c* Oxidase: A Time-Resolved Step-Scan Fourier Transform Infrared Study

Constantinos Koutsoupakis, Tewfik Soulimane, and Constantinos Varotsis

J. Am. Chem. Soc., **2003**, 125 (48), 14728-14732• DOI: 10.1021/ja036107e • Publication Date (Web): 06 November 2003

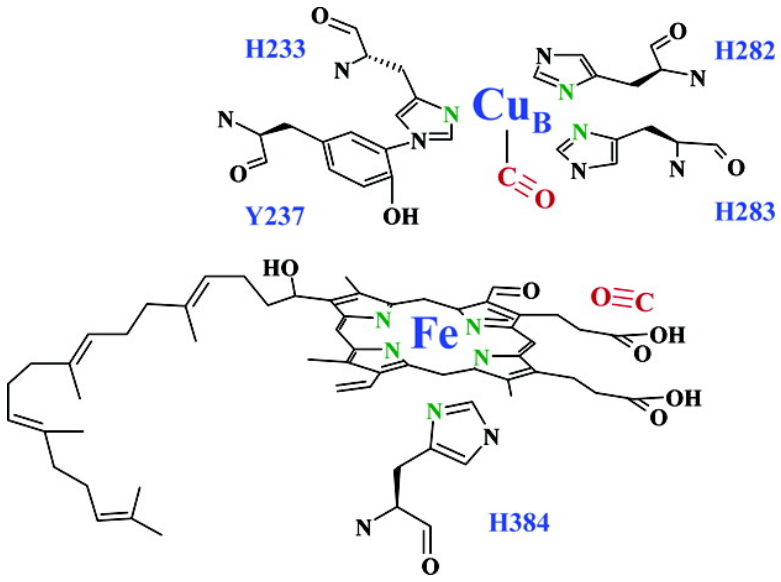

More About This Article

Additional resources and features associated with this article are available within the HTML version:

- Supporting Information
- Links to the 3 articles that cite this article, as of the time of this article download
- Access to high resolution figures
- Links to articles and content related to this article
- Copyright permission to reproduce figures and/or text from this article

View the Full Text HTML

J|A|C|S
ARTICLES
Published on Web 11/06/2003

Ligand Binding in a Docking Site of Cytochrome *c* Oxidase: A Time-Resolved Step-Scan Fourier Transform Infrared Study

Constantinos Koutsoupakis,[†] Tewfik Soulimane,[‡] and Constantinos Varotsis*,[†]

Contribution from the Department of Chemistry, University of Crete, 71409 Heraklion, Crete, Greece, and Paul Scherrer Institut, Life Sciences, OSRA/008,CH-5232 Villigen PSI, Switzerland

Received May 13, 2003; E-mail: varotsis@edu.uoc.gr

Abstract: The description of reaction regulation in enzymes responsible for activating and catalyzing small molecules (O_2, NO) requires identification of ligand movement into the binding site and out of the enzyme through specific channels and docking sites. We have used time-resolved step-scan Fourier transform infrared spectroscopy on CO-photolyzed cytochrome *c* oxidase ba_3 from *T. thermophilus*, which is responsible for the activation and reduction of both O_2 and NO, to gain insight into the structure of ligand-binding intermediates at ambient temperature. We show that, upon dissociation, the photolyzed CO becomes trapped within a ligand docking site located near the ring A propionate of heme a_3. The 2131 cm^{-1} mode of the "docked" CO we have detected corresponds to the B_1 state of Mb and persists for 35 μs. The release of CO from the docking site is not followed by recombination to the heme a_3 Fe. Our analysis indicates that this behavior reflects a mechanism in which the protein near ring A of heme a_3 propionate reorganizes about the released CO from the docking site, and establishes a transient barrier that inhibits the recombination process to the heme a_3 Fe for a few milliseconds. Rebinding to heme a_3 occurs with $k_2 = 29.5\ s^{-1}$. These results have implications for understanding the role of ligand binding/escape through docking sites and channels in heme-copper oxidases and, thus, in respiration.

Introduction

The structure determination of ligand binding intermediates in proteins and enzymes is the key step toward our understanding of ligand binding and discrimination. All proteins contain internal cavities that are coated by hydrophobic residues. The existence of these internal cavities, despite the reduced stability that they introduced to the protein, is explained by the general view of their involvement in controlling the dynamics and reactivity of the protein reactions with small ligands, such as O_2, NO, and CO, usually through ligand accommodation. On this point, many studies have been carried out on myoglobin, exploring the role of the internal cavities in controlling CO migration to the heme iron, and dictating internal pathways between the binding site and the transiently occupied docking sites.[1−15] The initial locations of photodissociated ligands in Mb are well established by ultrafast spectroscopic experiments[1,9] and theory.[2,14] The process of ligand docking and, thus, the direct observation of intermediate states have never been reported in other proteins or enzymes other than Mb and Hb.

Almost 95% of the oxygen we consume is used in respiration by the terminal respiratory enzyme cytochrome oxidase.[16] This remarkable machine, binds, activates, and reduces up to 250 molecules of O_2 per second, and couples the energy released in this process to the translocation of protons that contribute to the chemiosmotic gradient. Cytochrome ba_3 is a member of the large family of heme-copper oxidases and, in addition to activating O_2 and conserving the energy of the O_2 reduction for subsequent ATP synthesis, is able to catalyze the reduction of nitric oxide (NO) to nitrous oxide (N_2O) under reducing anaerobic conditions.[17] The crystal structure of the protein indicates that the conserved to all heme-copper oxidases subunit I consists of a low-spin heme *b* and a high-spin heme a_3/Cu_B binuclear center, where the dioxygen and nitric oxide reactions take place.[18] Subunit II contains a mixed valence homodinuclear

[†] University of Crete.
[‡] Paul Scherrer Institut.

(1) Lim, M.; Jackson, T. A.; Anfinrud, P. A. *Science* **1995**, *269*, 962−966.
(2) Elber, R.; Karplus, M. *Science* **1987**, *235*, 318−321.
(3) Moore, J. N.; Hansen, P. A.; Hochstrasser, R. M. *Proc. Natl. Acad. Sci. U.S.A.* **1988**, *85*, 5062−5066.
(4) Frauenfelder, H.; Sligar, S. G.; Wolynes, P. G. *Science* **1991**, *254*, 1598−1603.
(5) Ostermann, A.; Waschipky, R.; Parak, F. G.; Nienhaus, G. U. *Nature* **2000**, *404*, 205−208.
(6) Frauenfelder, H.; McMahon, B. H.; Austin, R. H.; Chu, K.; Groves, J. T. *Proc. Natl. Acad. Sci. U.S.A.* **2001**, *98*, 2370−2374.
(7) Austin, R. H.; Beeson, K. W.; Eisenstein, L.; Frauenfelder, H.; Gunsalus, I. C. *Biochemistry* **1975**, *14*, 5355−5373.
(8) Lamb, D. C.; Nienhaus, K.; Arcovito, A.; Draghi, F.; Miele, A. E.; Brunori, M.; Nienhaus, G. U. *J. Biol. Chem.* **2002**, *277*, 11636−11644.
(9) Moffat, K. *Nat. Struct. Biol.* **1998**, *5*, 641−643.
(10) Olson, J. S.; Phillips, G. N., Jr. *J. Biol. Chem.* **1996**, *271*, 17593−17596.
(11) Sagnella, D. E.; Straub, J. E.; Jackson, T. A.; Lim, M.; Anfinrud, P. A. *Proc. Natl. Acad. Sci. U.S.A.* **1999**, *96*, 14324−14329.
(12) Vitkup, D.; Petsko, G. A.; Karplus, M. *Nat. Struct. Biol.* **1997**, *4*, 200−206.
(13) Chu, K.; Ernst, R. M.; Frauenfelder, H.; Mourant, J. R.; Nienhaus, G. U.; Philipp, R. *Phys. Rev. Lett.* **1995**, *74*, 2607−2610.
(14) Meller, J.; Elber, R. *Biophys. J.* **1998**, *74*, 789−802.
(15) Lian, T.; Locke, B.; Kitagawa, T.; Nagai, M.; Hochstrasser, R. M. *Biochemistry* **1993**, *32*, 5809−5814.
(16) Varotsis, C.; Zhang, Y.; Appelman, E. H.; Babcock, G. T. *Proc. Natl. Acad. Sci. U.S.A.* **1993**, *90*, 237−241.
(17) Giuffrè, A.; Stubauer, G.; Sarti, P.; Brunori, M.; Zumft, W. G.; Buse, G.; Soulimane, T. *Proc. Natl. Acad. Sci. U.S.A.* **1999**, *96*, 14718−14723.

10.1021/ja036107e CCC: $25.00

Scheme 1

$$Fe^{2+}\,Cu_B^{+} + CO \underset{k_{-1}}{\overset{k_1}{\rightleftharpoons}} \underset{\mathbf{A}}{Fe^{2+},\,Cu_B^{+}\text{-}CO} \underset{k_{-2}}{\overset{k_2}{\rightleftharpoons}} \underset{\mathbf{B}}{Fe^{2+}\text{-}CO,\,Cu_B^{+}}$$

copper complex. The crystal structures of bovine aa_3,[19] *P. denitrificans* aa_3,[20] and *E. coli* bo_3[21] are also known, and most of the chemistry of heme-copper oxidases is understood. In addition, the coherent reaction dynamics has been recently reported for the bacterial cytochrome *c* oxidase.[22] Despite this wealth of knowledge, the actual chemical and structural details of proton translocation are still unknown, and very little is yet known about the ligand input and output channels and the docking sites in heme-copper oxidases. The CO-ligation/release mechanism in cytochrome ba_3 follows that found in other heme-copper oxidases[23] and proceeds according to Scheme 1.

In contrast to the bovine aa_3 oxidase, Cu_B of cytochrome ba_3 has a relative high affinity for CO ($K_1 > 10^4$), whereas the transfer of CO to heme $a_3{}^{2+}$ is characterized by a small $k_2 = 8$ s^{-1}, and by a $k_{-2} = 0.8$ s^{-1} that is 30-fold greater than that of the bovine aa_3.[24] It should be noted that the $Cu_B{}^{1+}-CO$ complex (complex **A**) is not photolabile, and thus it remains a spectator in the photodynamic events occurring to complex **B**.[25]

Mb has served as a model system toward our understanding of the interrelationships among structure, dynamics, and function in heme proteins.[26] In the photolyzed state of Mb, the "docked" CO is located in the distal site of the heme,[27,28] whereas in the photorelaxed state it is located in a proximal docking site.[29] The ultrafast time-resolved mid-IR dynamic experiments on Mb have revealed two trajectories of the CO within a distal docking site, but with opposite orientations, the B_1 (2131 cm^{-1}) and B_2 (2119 cm^{-1}) states, that are distinguished spectroscopically and kinetically.[30] Because of the importance of identifying the ligand binding entry and the product escape in heme-copper oxidases, we have continued our time-resolved step-scan FTIR spectroscopy (TRS^2) approach to heme-copper oxidases[31−34] and have identified the primary ligand intermediate in cytochrome ba_3 from *T. thermophilus*. This is the first study, other than those of Mb and Hb, where the process of ligand docking that represents the ligand escape pathway along with ligand binding pathway is used to describe the intermediate states occupied during conformational transitions in a large enzyme such as cytochrome ba_3. The "docked" CO at 2131 cm^{-1} is located near ring A of heme a_3 propionate that is 4.2 Å away from the heme a_3 Fe.[18]

Materials and Methods

Time-Resolved Step-Scan FTIR Spectroscopy. FTIR measurements were performed on a BRUKER Equinox IFS 55 spectrometer equipped with the step-scan option. The 532 nm pulses from a Continuum Minilite Nd:YAG laser (7 ns width, 3 Hz) were used as a pump light (4 mJ/pulse) to photolyze the ba_3-CO oxidase. The transient populations of the $Cu_B{}^{1+}-CO$ complex and of "docked" CO were generated by photolyzing approximately 15% of the heme $a_3{}^{2+}-CO$ complex. For the time-resolved experiments, a TTL pulse (Transistor Transistor Logic) provided by a digital delay pulse generator (Quantum Composers, 9314T) triggers, in order, the flashlamps, Q-switch, and the FTIR spectrometer. Pretriggering the FTIR spectrometer to begin data collection before the laser fires allows 40−100 fixed reference points to be collected at each mirror position, which are averaged and used as the reference spectrum in the calculation of the difference spectra. Changes in intensity were recorded with an MCT detector (Mercury Cadmium Telluride, Graseby Infrared D316, response limit 600 cm^{-1}) amplified in the dc-coupled mode and digitized with a 200-kHz, 16-bit, analog-to-digital converter. A broad-band interference optical filter (Optical Coating Laboratory, Santa Rosa, CA) with short wavelength cutoff at 2.67 μm was used to limit the free spectral range from 2.67 to 8 μm. This leads to a spectral range of 3949.5 cm^{-1}, which is equal to an undersampling ratio of 4. Single-sided spectra were collected at 8 cm^{-1} spectral resolution (1110 mirror positions), 5 or 100 μs time-resolution, and 10 coadditions per data point. The total accumulation time for each measurement was 62 min, and 2−3 measurements were collected and averaged. The Blackman−Harris three-term apodization function with 32 cm^{-1} phase resolution and the Mertz phase correction algorithm were used. Difference spectra were calculated by subtracting the reference spectrum, recorded before the laser firing, from those after the photodissociation of CO from heme a_3. In the spectral region between 1900 and 2150 cm^{-1}, the noise level was 10^{-5} AU.

Sample Preparation. Cytochrome ba_3 was isolated from *T. thermophilus* HB8 cells according to previously published procedures.[24] The samples used for the FTIR measurements had an enzyme concentration of ~1 mM and were placed in MES buffer (pH 5.25). Dithionite-reduced samples were exposed to 1 atm CO (1 mM) in an anaerobic cell to prepare the carbonmonoxy adduct and transferred to a tightly sealed FTIR cell composed of two 3-mm-thick CaF_2 windows, under anaerobic conditions. The path length was sufficient small (15 μm) to avoid the strong absorbance of the water around 1650 cm^{-1} and keep the response of the MCT detector linear. The enzyme binds CO homogeneously to the catalytic center at pH 5.25 for a time period much longer (10−12 h) than the corresponding time for sample preparation and measurement. CO gas (99.9%) was obtained from Messer (Germany). Optical absorption spectra were recorded with a Perkin-Elmer Lamda 20 UV−visible spectrometer before and after the FTIR measurements to ensure the formation and stability of the CO adducts.

Results and Discussion

Location of Ligand Docking Site. Figure 1 shows the TRS^2 difference spectra ($t_d = 5-60$ μs, 8 cm^{-1} spectral resolution) of fully reduced ba_3-CO after CO photolysis by a nanosecond laser pulse (532 nm). The negative peak at 1976 cm^{-1} arises

(18) Soulimane, T.; Buse, G.; Bourenkov, G. P.; Bartunik, H. D.; Huber, R.; Than, M. E. *EMBO J.* **2000**, *19*, 1766−1776.
(19) Yoshikawa, S.; Shinzawa-Itoh, K.; Nakashima, R.; Yaono, R.; Yamashita, E.; Inoue, N.; Yao, M.; Fei, M. J.; Libeu, C. P.; Mizushima, T.; Yamaguchi, H.; Tomizaki, T.; Tsukihara, T. *Science* **1998**, *280*, 1723−1729.
(20) Ostermeier, C.; Harrenga, A.; Ermler, U.; Michel, H. *Proc. Natl. Acad. Sci. U.S.A.* **1997**, *94*, 10547−10553.
(21) Abramson, J.; Riistama, S.; Larsson, G.; Jasaitis, A.; Svensson-Ek, M.; Laakkonen, L.; Puustinen, A.; Iwata, S.; Wikstrom, M. *Nat. Struct. Biol.* **2000**, *7*, 910−917.
(22) Liebl, U.; Lipowski, G.; Nigrerie, M.; Lambry, J.-C.; Martin, J.-L.; Vos, M. H. *Nature* **1999**, *401*, 181−184.
(23) Woodruff, W. H. *J. Bioenerg. Biomembr.* **1993**, *25*, 177−188.
(24) Giuffrè, A.; Forte, E.; Antonini, G.; D'Itri, E.; Brunori, M.; Soulimane, T.; Buse, G. *Biochemistry* **1999**, *38*, 1057−1065.
(25) Alben, J. O.; Moh, P. P.; Fiamingo, F. G.; Altschuld, R. A. *Proc. Natl. Acad. Sci. U.S.A.* **1981**, *78*, 234−237.
(26) Mizutani, Y.; Kitagawa, T. *Science* **1997**, *278*, 443−446.
(27) Hartmann, H.; Zinser, S.; Komninos, P.; Schneider, R. T.; Nienhaus, G. U.; Parak, F. *Proc. Natl. Acad. Sci. U.S.A.* **1996**, *93*, 7013−7016.
(28) Schlichting, I.; Berendzen, J.; Phillips, G. N., Jr.; Sweet, R. M. *Nature* **1994**, *371*, 808−812.
(29) Chu, K.; Vojtchovsky, J.; McMahon, B. H.; Sweet, R. M.; Berendzen, J.; Schlichting, I. *Nature* **2000**, *403*, 921−923.
(30) Lim, M.; Jackson, T. A.; Anfinrud, P. A. *Nat. Struct. Biol.* **1997**, *4*, 209−214.
(31) Koutsoupakis, K.; Stavrakis, S.; Pinakoulaki, E.; Soulimane, T.; Varotsis, C. *J. Biol. Chem.* **2002**, *277*, 32860−32866.
(32) Pinakoulaki, E.; Soulimane, T.; Varotsis, C. *J. Biol. Chem.* **2002**, *277*, 32867−32874.
(33) Stavrakis, S.; Koutsoupakis, K.; Pinakoulaki, E.; Urbani, A.; Saraste, M.; Varotsis, C. *J. Am. Chem. Soc.* **2002**, *124*, 3814−3815.
(34) Koutsoupakis, K.; Stavrakis, S.; Soulimane, T.; Varotsis, C. *J. Biol. Chem.* **2003**, *278*, 14893−14896.

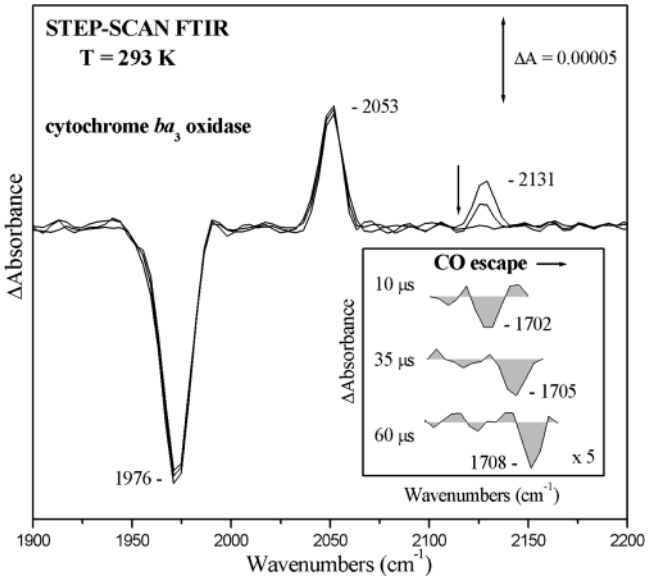

Figure 1. Time-resolved step-scan FTIR difference spectra of the CO-bound form of fully reduced cytochrome ba_3 oxidase (pH 5.25) at 10, 35, and 60 μs after CO photolysis. Enzyme concentration was ~1 mM, and the path length was 15 μm. Each spectrum is the average of 5−10 individual spectra. The spectral resolution was 8 cm^{-1}, the time resolution was 5 μs, and 10 coadditions were collected per data point. The excitation wavelength was 532 nm (4 mJ/pulse). Inset: Time-resolved step-scan FTIR difference spectra (1675−1720 cm^{-1} spectral region) of the cytochrome ba_3−CO complex at 10, 35, and 60 μs after CO photolysis. Each spectrum is the average of 5−10 individual spectra, and the experimental conditions were the same as those described above.

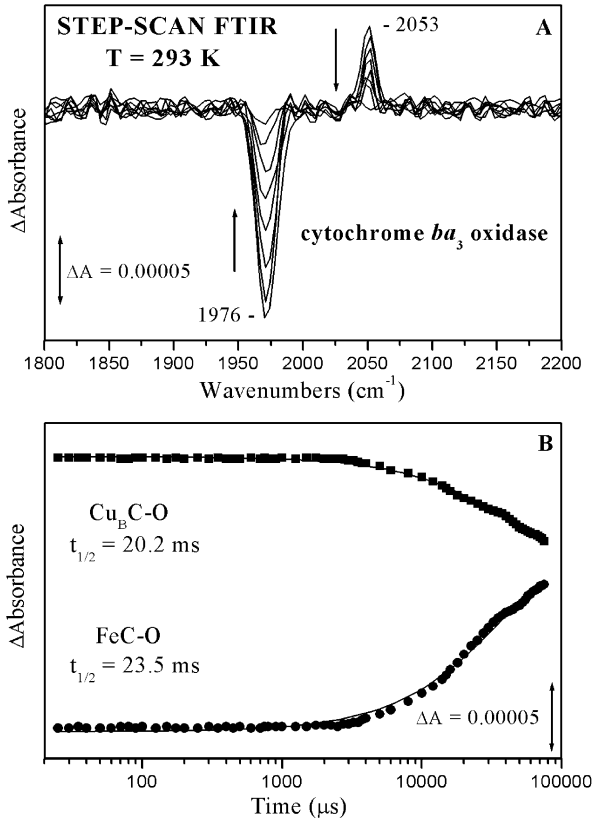

Figure 2. (A) Time-resolved step-scan FTIR difference spectra of the CO-bound form of fully reduced cytochrome ba_3 oxidase (pH 5.25) at 1, 5, 10, 20, 40, 60, 75, and 100 ms after CO photolysis. Each spectrum is the average of 40 individual spectra. (B) Kinetic analysis of the 2053 cm^{-1} (Cu_BC−O) (■) and 1976 cm^{-1} (FeC−O) (●) modes versus time, after CO photolysis. ΔA was measured from the intensity of the corresponding modes (peaks area), at times between 0 and 75 ms, after the photolysis of CO from heme a_3. The curves are three-parameter exponential fits to the experimental data, according to first-order kinetics.

from the photolyzed heme a_3−CO, and the positive peak that appears at 2053 cm^{-1} is the result of the photolyzed CO that transiently binds to Cu_B. Concurrently with the formation of the Cu_B^{1+}−CO complex, a positive peak appears at 2131 cm^{-1} that shows a slight evolution as it diminishes at ~60 μs. The TRS[2] difference spectra presented here, in conjunction with the reported extinction coefficients for heme a_3−CO and Cu_B^{1+}−CO,[25] demonstrate that 80−85% of the photodissociated CO binds to Cu_B. The remaining 15−20% is attributed to the population of the 2131 cm^{-1} mode (see below). The frequency of the 2131 cm^{-1} feature is close to the free-gas value of CO (2143.3 cm^{-1})[35] and exactly the same as that found in Mb, characterizing the B_1 state in which the CO is trapped into a docking site located above the pyrrole ring C of the heme.[27−30] Accordingly, we assign the 2131 cm^{-1} mode we observe in the photolyzed ba_3 to the B_1 state in which the CO is funneled into a docking site. We cannot exclude, however, the possibility that both B_1 (2131 cm^{-1}) and B_2 (2119 cm^{-1}) states are initially formed after CO photodetachment from heme a_3 and that B_1 becomes dominant at the time of our time-resolution limitations (5 μs). No significant intensity variations are detected in the transient difference spectra (t_d = 5−3000 μs) for the 2053 and 1976 cm^{-1} modes. The "docked" CO escapes within 60 μs without rebinding to heme a_3 or Cu_B. Concurrently with the decay of the 2131 cm^{-1} mode, the propionate C═O stretching band of ring A of heme a_3 is seen as a negative peak at 1708 cm^{-1} (Figure 1, inset).[31] Prior to the decay of the "docked" CO, however, it is observed at 1702 cm^{-1} at t_d = 10 μs, and at 1705 cm^{-1} (t_d = 35 μs). This observation indicates that the "docked" CO is near the C═O stretching band of the ring A propionate of heme a_3, causing a conformational change to the C═O bond. When the "docked" CO escapes, the heme propionate is free of the exerted perturbation and returns progressively from its transient position at 1702 to 1708 cm^{-1}. We cannot exclude, however, that there are more than two states involved in the 1702 to 1708 cm^{-1} transition. It should be noted that the C═O bond is located at 1708 cm^{-1} during the entire CO rebinding process to heme a_3. This observation further supports our conclusion that the frequency of the 1702 cm^{-1} mode is due to the presence of the "docked" CO near ring A of heme a_3 propionate, and is not the consequence of CO photodissociation from heme a_3. If the later scenario was the case, then a similar perturbation in the C═O mode would have been observed during the rebinding process. No such perturbation of the C═O mode, however, was observed. The inset shows the time evolution of the ring A heme a_3 propionate.

At t_d = 3−100 ms (Figure 2A), the decreased intensity of the transient 2053 cm^{-1} mode is accompanied by an increased intensity at 1976 cm^{-1}. The final spectrum at 100 ms demonstrates that there is no irreversible light-induced effect on heme a_3. The intensity ratio of Fe−CO/Cu_B−CO remains constant for all data points (~2.0), and thus we conclude that no fraction of CO that was bound to Cu_B escapes the binuclear center at 293 K. On the basis of the final intensity of the 1976 cm^{-1} mode, we further conclude that the "docked" CO that was not bound to Cu_B has recombined to heme a_3. Figure 2B compares

(35) Lim, M.; Jackson, T. A.; Anfinrud, P. A. *J. Chem. Phys.* **1995**, *102*, 4355−4366.

Scheme 2

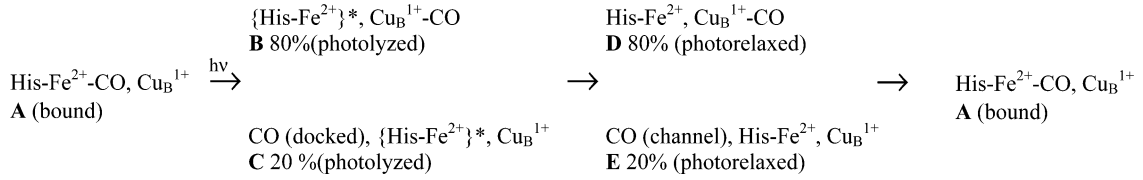

the decay of the $Cu_B^{1+}-CO$ complex, as measured by the ΔA of the 2053 cm^{-1} mode shown in Figure 2A, with the formation of the heme $a_3^{2+}-CO$ complex by measuring the ΔA of the 1976 cm^{-1} mode. The rate of decay of the transient $Cu_B^{1+}-CO$ complex is 34.3 s^{-1} ($t_{1/2} = 20.2$ ms), and the observed rate of rebinding to heme a_3 is 29.5 s^{-1} ($t_{1/2} = 23.5$ ms). The presented curves are three-parameter fits to the experimental data and show that the kinetics of the transient species is similar to that previously obtained at pD 8.5.[31]

Photodissociation Dynamics. In Scheme 2, we present a model for CO kinetics, heme-pocket relaxation, and coordination chemistry in the heme a_3-Cu_B binuclear center of ba_3.

We expect the same time scales for the initial events in the photodynamics of cytochrome ba_3 as those reported for mammalian aa_3 oxidase.[23,36] Therefore, the $Cu_B^{1+}-CO$ complex is fully developed within 1 ps after CO photolysis from heme a_3, demonstrating the absence of activation barrier to the CO transfer from heme a_3 to Cu_B.[37] The states denoted by an asterisk (**B** and **C**) represent a nonequilibrium heme a_3 state characterized by an upshifted heme a_3 Fe−His stretching vibration that relaxes to the equilibrium reduced species at times >10 μs.[36,38,39] In states **B** and **C**, the photolyzed CO and the heme pocket contain excess energy resulting from the photolysis. The produced heat from the energy of the 532 nm photons appears as excess translational and rotational energy of the CO, without being vibrationally excited, and as an excess energy in the binuclear moiety. The activated CO (80−85%) binds to Cu_B, and the other 15−20% is funneled in the "docking" site before the binuclear center is thermalized. In state **E**, the "docked" CO has escaped from its original position, and in state **A** both the solvated CO and that bound to Cu_B rebind to heme a_3. It is expected that the docking site that traps the photolyzed CO be able to trap the thermally dissociated CO from Cu_B, an event that occurs with $t_{1/2} = 20.2$ ms. However, we detect no signals at 2131 cm^{-1} during the thermal dissociation of CO from Cu_B.

The TRS^2 difference spectra demonstrate that the docking site is near ring A of heme a_3 propionate and remains there for 35 μs. The lack of recombination of the "docked" CO to heme a_3 in conjunction with the absence of CO escape from the binuclear center indicates that the original "docking" site barrier (5−35 μs) to recombination, that is formed with photodissociation of CO, is followed by a second transient barrier (35 μs to 3 ms). We suggest that this second barrier is the result of the long-lifetime of the "docked" CO that causes large-scale protein fluctuations on microseconds to milliseconds time scales, and concomitantly creates a transient protein channel near the binuclear center. Evidently, the escaped "docked" CO becomes solvated and remains trapped in the transient channel. Unfortunately, the intensity of the solvated CO mode (B_0 state),[40] at ~2146 cm^{-1}, is by a factor of ~50[41] lower than that representing the ligated form and, thus, beyond our detection limits. Protein fluctuations have also been observed in Mb, whereas the recombination of CO from the docking site to the heme is slowed substantially, allowing a large fraction of ligands to avoid rebinding long enough.[8,29] This way, large-scale fluctuations on nanosecond to microsecond time scales open exit channels through which ligands migrate into other internal cavities from which they finally escape from the protein. Obviously, in cytochrome ba_3, the protein fluctuations are not followed by the creation of new docking sites or exit channels from which ligands escape. Accordingly, the heme a_3 Fe−His relaxation, the dynamics of the docking site, and that of the transient channel are the rate-limiting steps to geminate recombination.

Physiological Relevance. It is anticipated that the same docking site is responsible for the kinetic control of both ligand motion/binding and escape and that ba_3 has preexisting cavities that are only modestly perturbed by the photodissociated CO from heme a_3. The experimental observation of the putative ligand binding intermediate state **C** (Scheme 2) in heme-copper oxidases can be used to evaluate the ligand input and escape pathways. The results reported here in conjunction with those reported on the protonic connectivity between the propionates of heme a_3, Asp372, and H_2O, that lead to the identification of a proton exit channel, indicate a pathway connecting the docking and binding sites and indicate that this pathway leads to the escape of protons and H_2O molecules (Koutsoupakis, C.; Soulimane, T.; Varotsis, C. *Biophys. J.*, submitted).

Combining the results above with those of photodissociated Mb, the following points emerge. Upon photodissociation from heme a_3, 15−20% of CO becomes trapped in a docking site that is located at ring A of heme a_3 propionate. The protein environment near ring A of heme a_3 propionate imposes constraints on the released CO from the docking site, preventing its fast rebinding to heme a_3. In a broader sense, our results highlight the emerging general strategy of heme proteins, which function either as ligand carriers or as catalytic enzymes. In Mb, the docking sites are transiently occupied by the ligand during its trajectory though the protein. This way, the pathway for migration to and from the active center is defined. As for cytochrome ba_3, the identification of the docking site near ring A of heme a_3 propionate provides the basis for subsequent analysis of its functional role in the reductions of O_2 to H_2O and of NO to N_2O.[17] Given the similar size and polarity of CO and O_2, O_2 migration to the docking site is expected. This way, the long-lived "docked" ligand may participate in chemical

(36) Findsen, E. W.; Centeno, J.; Babcock, G. T.; Ondrias, M. R. *J. Am. Chem. Soc.* **1987**, *109*, 5367−5372.
(37) Dyer, R. B.; Peterson, K. A.; Stoutland, P. O.; Woodruff, W. H. *J. Am. Chem. Soc.* **1991**, *113*, 6276−6277.
(38) Varotsis, C.; Babcock, G. T. *J. Am. Chem. Soc.* **1995**, *117*, 11260−11269.
(39) Schelvis, J. P. M.; Deinum, G.; Varotsis, C.; Fergusson-Miller, S.; Babcock, G. T. *J. Am. Chem. Soc.* **1997**, *119*, 8409−8416.
(40) Alben, J. O.; Beece, D.; Bowne, S. F.; Doster, W.; Eisenstein, L.; Frauenfelder, H.; Good, D.; McDonald, J. D.; Marden, M. C.; Moh, P. P.; Reinisch, L.; Reynolds, A. H.; Shyamsunder, E.; Yue, K. T. *Proc. Natl. Acad. Sci. U.S.A.* **1982**, *79*, 3744−3748.
(41) Anfinrud, P. A.; Han, C.; Hochstrasser, R. M. *Proc. Natl. Acad. Sci. U.S.A.* **1989**, *86*, 8387−8391.

reaction, as it has been demonstrated in the reaction mechanism of the $Mb-O_2$ and $Hb-O_2$ with NO.[42] The spectroscopic identification of the docking site presented here, in conjunction with time-resolved Laue X-ray diffraction data,[43] will provide a framework for elucidating the reaction pathways in cytochrome oxidase.[44]

Acknowledgment. We thank Stavros Stavrakis for excellent technical assistance and Dr. Eftychia Pinakoulaki for helpful discussions. This work was partially supported by the Greek Ministry of Education.

JA036107E

(42) Eich, R. F.; Li, T.; Lemon, D. D.; Doherty, D. H.; Curry, S. R.; Aitken, J. F.; Mathews, A. J.; Johnson, K. A.; Smith, R. D.; Phillips, G. N., Jr.; Olson, J. S. *Biochemistry* **1996**, *35*, 6976−6983.

(43) Srajer, V.; Teng, T.-y.; Ursby, T.; Pradervand, C.; Ren, Z.; Adachi, S.-i.; Schildkamp, W.; Bourgeois, D.; Wulff, M.; Moffat, K. *Science* **1996**, *274*, 1726−1729.

(44) Koutsoupakis, C.; Soulimane, T.; Varotsis, C. *J. Biol. Chem.* **2003**, *278*, 36806−36809.